Hindawi
Journal of Applied Mathematics
Volume 2022, Article ID 9071890, 14 pages
https://doi.org/10.1155/2022/9071890

Research Article

Mathematical Modelling and Optimal Control Strategies of a Multistrain COVID-19 Spread

Bouchaib Khajji,[1] **Lahoucine Boujallal**,[2] **Omar Balatif**,[3] **and Mostafa Rachik**[1]

[1]*AMS Laboratory, FS Ben M'Sik, Hassan II University, Sidi Othman, Casablanca, Morocco*
[2]*LMFA Laboratory, FS Ain Chock, Hassan II University, Casablanca, Morocco*
[3]*DS Laboratory, FS El Jadida, Chouaib Doukkali University, El Jadida, Morocco*

Correspondence should be addressed to Bouchaib Khajji; khajjibouchaib@gmail.com

Received 21 April 2021; Revised 10 February 2022; Accepted 28 June 2022; Published 16 July 2022

Academic Editor: Frank Werner

In this paper, we propose a continuous mathematical model that describes the spread of multistrains COVID-19 virus among humans: susceptible, exposed, infected, quarantined, hospitalized, and recovered individuals. The positivity and boundedness of the system solution are provided in order to get the well posedness of the proposed model. Secondly, three controls are considered in our model to minimize the multistrain spread of the disease, namely, vaccination, security campaigns, social distancing measures, and diagnosis. Furthermore, the optimal control problem and related optimality conditions of the Pontryagin type are discussed with the objective to minimize the number of infected individuals. Finally, numerical simulations are performed in the case of two strains of COVID-19 and with four control strategies. By using the incremental cost-effectiveness ratio (ICER) method, we show that combining vaccination with diagnosis provides the most cost-effective strategy.

1. Introduction

In late 2019, coronavirus (COVID-19) outbreak occurred in the Chinese city of Wuhan and then spread to most countries of the world. The virus caused the infection and death of millions. Consequently, several countries have had to resort to the quarantine strategy, which is based on preventing the movement of people and animals from countries suffering from this disease. It also consists of establishing control points to prevent and regulate exit and entry in areas affected by the pandemic with the imposition of a health emergency in all countries of the world to limit the spread of COVID-19. After taking such measures, the number of infections and deaths decreased, but the quarantine strategy has greatly affected the global economy and made it shrink [1]. Domestic violence, unemployment, and psychological problems increased, especially for the elderly with disabilities and chronic diseases like diabetes, hypertension, and cardiovascular disease. These health problems are important risk factors for severity and mortality in people infected with COVID-19 [2].

The COVID-19 virus mutated and induced a second strain, SARS-CoV-2 VOC, that appeared on December 14, 2020, initially in South-East England. The UK authorities informed the World Health Organization of a variant named by the United Kingdom as SARS-CoV-2 VOC 202012/01. The number of COVID-19 infections rose rapidly as well as hospital admissions in England in December after a decrease in infections in late November. Thus, an estimation of 1,122,000 people in England, or 1 in 50 people, was infected with COVID-19 in the first week of January 2021. This number accounts for 2.06% of the population and is more than twice the positivity rate recorded in the first week of December 2020, when 0.88% of the population were estimated to have the virus. The number of hospitalized people with COVID-19 also rose in the first week of January 2021 to

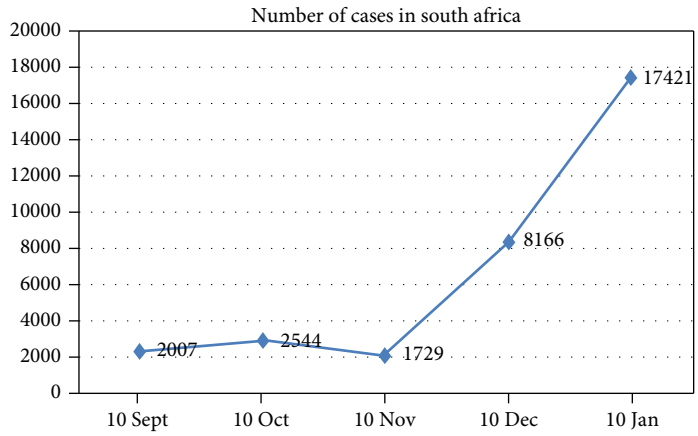

(a) Number of cases in South Africa

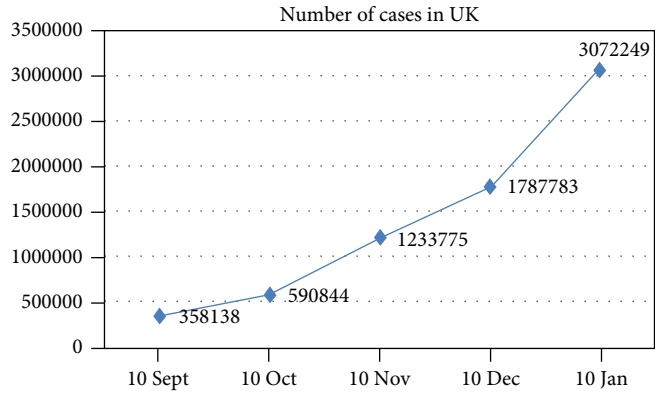

(b) Number of cases in UK

Figure 1: Schematic diagram of the total confirmed cases in the UK and South Africa.

27.8 admissions per 100,000 people. This is almost twice the rate seen in the first week of December 2020, of 14 per 100,000 people, 8 January 2021 [3].

Following England, South Africa's national authorities announced on December 18 the outbreak of a new type of SARS-CoV-2 virus described by rapid spreading in three provinces of South Africa. South Africa gave the name 501Y.V2 to this variant, due to the N501Y mutation. SARS-CoV-2 VOC 2012/01 originated in the UK also has the N501Y mutation. Phylogenetic analysis showed that 501Y.V2 from South Africa is a different viral variant. In the third week of November 16, after conducting routine sequencing, South African health authorities concluded that this new variant of SARS-CoV-2 had largely supplanted other SARS-CoV-2 viruses existing in the Eastern Cape provinces, the Western Cape, and KwaZulu-Natal. While the genomic data demonstrated that the 501.V2 variant displaced other strains circulating in South Africa in a fast pace, preliminary studies indicate that the variant is associated with a higher viral load, which may refer to the possibility of increased transmissibility. Other factors having impact on transmissibility are also under investigation. Thorough studies are still needed to understand the new variant's effect on transmission, clinical severity of infection, laboratory diagnosis, treatments, vaccinations, or public health preventive measures [3].

The WHO confirmed that since it was first reported on Dec. 14, the mutated virus discovered by Britain has been announced in 50 countries, territories, and regions. The strain that was found in South Africa and first reported on December 18 exists up to now in 20 countries. The United Nations has expressed concern over the new variants like Alpha, Beta, Gamma, and Delta. These variants may have a serious effect on the immune response and need more investigation according to the organization. Indeed, the virus dissemination means it is more likely to mutate. Also, the high levels of transmission lead to the emergence of more strains [3].

Since COVID-19 transmission continues and the number of infected people rises by the second strain, it was discovered that the virus affects all age groups. The new strain of COVID-19 happens to be detrimental for all people even if they are hospitalized due to the current pandemic. For example, data in Figure 1 demonstrate that the likelihood of infections from the disease rise with the second strain in the UK and South Africa [4, 5].

Consequently, many mathematical studies were suggested to apprehend different factors that can lead to a disease transmission and to decide on the future control strategies to eradicate the disease. For example, in [6], the authors have introduced a new modelling approach based on the account of the age structure and uses fractional-

order derivatives model, aiming to describe the transmission of COVID-19 and investigate the impact of some control strategies on its spread. The work done in [7] introduced a new approach of modelling based on a multiregion discrete time model that is composed of two groups: the human population and the animal population in different regions. It aimed to describe the spatial-temporal evolution of COVID-19 which appears in different geographical regions and showing the impact of one region on another. Moreover, they suggested several control strategies, including campaigns of awareness in a certain region, security campaigns, health measures to stop the movement of individuals from one region to another, and urging the individuals to join quarantine centers and the disposing of infected animals. In [8], the authors presented a mathematical model containing five compartments to depict the transmission evolution of the COVID-19 virus. The population is split into potential people, infected people without symptoms, people with serious complications, individuals under health surveillance and quarantined, and people who recovered from the disease. In addition, optimal control strategies were introduced, which include spreading awareness campaigns for citizens along with practical measures to limit the propagation of the virus including diagnosis of individuals, surveillance of airports, and imposing quarantine on infected people. Rahim et al. [9] have introduced a four compartments model for the description of the ongoing COVID-19. They have set up global and local dynamics for the established model. To decrease the number of infections and to minimize the cost of applying government control guidelines, an optimal control problem is formulated and solved in [10]. In [11], Ndii et al. proposed a deterministic and stochastic mathematical model to determine the probability of extinction of COVID-19 transmission. In addition, they calculated the proportion of undetected infected individuals and assessed the effectiveness of the following strategies: reducing the transmission rate and accelerating the detection time of infected persons. They found that the combination of the two strategies is effective in slowing outbreaks. They also found that accelerating the detection time of infected people without reducing the rate of transmission is not enough to slow epidemics.

Generally, the existing models in the literature vary on the choice of the compartmental model, on the constraints enforced, or on the functional cost. These models are generally governed by ordinary equations [11–16], partial [17, 18] and stochastic differential equations [11, 19, 20]. More recently, fractional differential equations are increasingly used to model several phenomena.

The above cited works, and the majority of models in the literature, did not take into consideration the possibility of multiple viral strain of COVID-19. However, multistrain models should be used to understand a mutated COVID-19 virus spreading into a population. Such models have been used in fewer studies, as in [21], where the authors investigated the global stability of two-strain SEIR model with two general incidence rates, and even for multistrain SEIR model with saturated incidence and treatment controls as in [22], which also deals with an optimal control problem. Local stability of multistrain SIR model with selective immunity by vaccination has been treated in [23]. The processes of mutation were also observed in many other infections such as tuberculosis [24–26]. Motivated by the relevance and scarcity of multistrain COVID-19 models, we intend to offer an extension of the classical models that describe the dynamics of COVID-19 with multistrains of infectious disease. Moreover, we propose some effective control strategies in order to minimize the infected individuals. More precisely, the main contributions of this paper are summarized as follows:

(i) Evolving an epidemic model taking into account multistrain characteristics of COVID-19 and evaluating the impact of certain control strategies

(ii) Offering a developed SEIR model, where the population is divided into $n+5$ compartments. Particularly, Susceptible (S), Exposed (L), Infectious with i -th strain of COVID-19 (I_i), where $i = 1, \cdots, n$, Hospitalized (H), Quarantined (Q), and Recovered (R) individuals

(iii) Seeking effective optimal control strategies that minimize the amount of infected population with symptoms of all strain types. To satisfy this objective, we introduce optimal control strategies related to three sorts of controls: the first control represents the density of susceptible individuals vaccinated per time unit; the second control represents the effort of the awareness programs, security campaigns, and social distancing measures to protect the susceptible individuals not to become infected. The third control is meant to encourage the infected individuals with strains of COVID-19 to join quarantine centers or go to hospitals

(iv) Providing numerical simulations in the case of two strains of COVID-19 along with a combination of the three control strategies. By using the incremental cost-effectiveness ratio (ICER) method, we prove that the combination of vaccination with diagnosis provides the most cost-effective strategy

The paper is organized as follows: In Section 2, we introduce a novel mathematical model that illustrates the dynamics of the population and the transmission of the strains of COVID-19 disease as well as the existence and uniqueness of solution of the model. In Section 3, we design the optimal control terms by using Pontryagin's maximum principle. While Section 4 discuss some numerical simulation results, and cost-effectiveness analysis is given in Section 5. Finally, we finish this paper in Section 6.

2. Multistrains COVID-19 Model and Analysis

2.1. Description of the Model. In this section, we describe the dynamics of the population and the transmission of the strains of COVID-19 disease. The population is grouped into $n+5$ compartments: Susceptible S, Exposed L, Infected

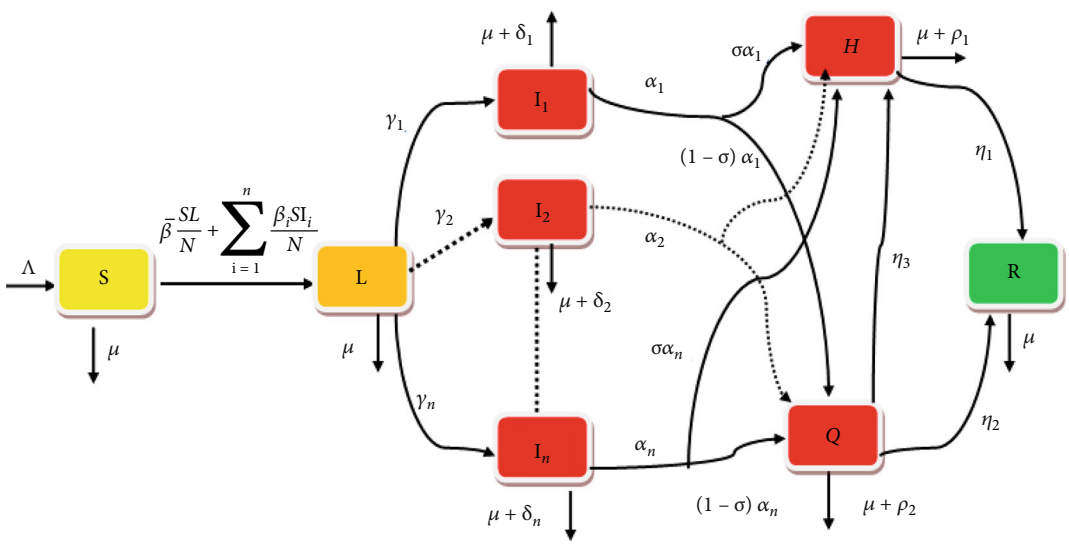

Figure 2: Illustrative design of the $n+5$ infectious classes in the population.

with i^{th} strain I_i, Hospitalized H, Quarantined Q, and Recovered R. In Figure 2, we build a graphical representation of the proposed model.

Then, the model can be governed by the following $n+5$ -ordinary differential equations:

$$\begin{cases} \dfrac{dS(t)}{dt} = \Lambda - \bar{\beta}\dfrac{S(t)L(t)}{N} - \displaystyle\sum_{i=1}^{n}\dfrac{\beta_i S(t)I_i(t)}{N} - \mu S(t), \\ \dfrac{dL(t)}{dt} = \bar{\beta}\dfrac{S(t)L(t)}{N} + \displaystyle\sum_{i=1}^{n}\dfrac{\beta_i S(t)I_i(t)}{N} - \left(\mu + \displaystyle\sum_{i=1}^{n}\gamma_i\right)L(t), \\ \dfrac{dI_i(t)}{dt} = \gamma_i L(t) - (\mu+\delta_i+\alpha_i)I_i(t), \text{for } i = 1, 2, \ldots \cdots, n, \\ \dfrac{dH(t)}{dt} = \displaystyle\sum_{i=1}^{n}\sigma\alpha_i I_i(t) - (\mu+\eta_1+\rho_1)H(t) + \eta_3 Q(t), \\ \dfrac{dQ(t)}{dt} = \displaystyle\sum_{i=1}^{n}(1-\sigma)\alpha_i I_i(t) - (\mu+\eta_2+\eta_3+\rho_2)Q(t), \\ \dfrac{dR(t)}{dt} = \eta_1 H(t) + \eta_2 Q(t) - \mu R(t), \end{cases} \tag{1a}$$

with initial states

$$\begin{aligned} &S(0) \geq 0, L(0) \geq 0, I_i(0) \geq 0, \\ &H(0) \geq 0, Q(0) \geq 0, R(0) \geq 0. \end{aligned} \tag{1b}$$

The compartment S: is the group of susceptible persons who are not infected but can get sick. The population is born into this compartment at a recruitment rate presented by Λ and gets infected by an effective contact with L at a rate $\bar{\beta}$, and with the infectious individuals I_i at β_i rate. It is also decreased by a natural death at a rate μ. It is assumed that susceptible individuals can become infectious through effective contact with infected individuals in workplace or house.

The compartment L: is composed of the exposed who are carriers of the virus without symptoms or with low symptoms and can spread the virus and become infected with symptoms. It is increased by susceptible S who becomes exposed at the rates $\bar{\beta}, \beta_1, \beta_2, \ldots \cdots, \beta_n$, This group is decreased by natural death at rate μ and when the exposed become infectious with symptoms at rates $\gamma_1, \gamma_2, \ldots \cdots$ and γ_n.

The compartment I_i: contains infectious individuals with symptoms and with a ith strain of corona. It becomes larger as the amount of the infectious individuals with symptoms and with a i strain of corona increase by the rate γ_i (γ_i is a rate the exposed individuals who get infected with symptoms) and decreases when some of them recovered at a rate α_i (α_i is a rate of the infected individuals with symptoms who are hospitalized or quarantined). Furthermore, this class decreases by natural death rate μ and by δ_i; the death rate of infectious person with i^{th} strains of COVID-19.

The compartment H: illustrates the individuals who join hospitals, where $\sigma\alpha_i$ denoted the recruitment rate of individuals and I_i who have joined hospitals. Some individuals in quarantine go to a hospital at a rate η_3 (η_3 is a rate of quarantined individuals who have been hospitalized) and decrease when they become recovered at a rate η_1 (a rate of the hospitalized individuals who have recovered). Furthermore, H decreases by natural death μ and by ρ_1 the death rate of infected individuals with COVID-19 in hospital.

The compartment Q: encompasses the individuals who have been quarantined, with $\sum_{i=1}(1-\sigma)\alpha_i$ is the recruitment rate of individuals who have infected with new strains of COVID-19. While η_2 represents a rate of the quarantine individuals that recovered and η_3 is a rate of the quarantine individuals that hospitalized. Also, the compartment Q

decreases by natural death μ and by ρ_2 the death rate of quarantined infected individuals.

The compartment R: consists of individuals group who recovered from COVID-19 virus, where parameters η_1 and η_2 are the recruitment rates of individuals (H and Q) who have been treated. Also, R is decreased by natural death μ.

Thus, the total population at time t is presented by

$$N(t) = S(t) + L(t) + \sum_{i=1}^{n} I_i(t) + H(t) + Q(t) + R(t). \quad (2)$$

2.2. Positivity and Boundedness of Solution. Motivated by the biological meaning of the mathematical model (1a), we prove, in this section, the positivity and boundedness of the solution of the system (1a) on a defined subset.

Lemma 1. *Assume that condition (1b) is satisfied, then the solution of system (1a) is positive for any time $t > 0$.*

Proof. From the system (1a), we have:

$$\frac{dS(t)}{dt} = \Lambda - \left[\bar{\beta}\frac{L(t)}{N} + \sum_{i=1}^{n}\frac{\beta_i I_i(t)}{N} + \mu\right] S(t). \quad (3)$$

By taking

$$M(t) \doteq \bar{\beta}\frac{L(t)}{N} + \sum_{i=1}^{n}\frac{\beta_i I_i(t)}{N} + \mu, \quad (4)$$

it follows from Equation (3) that

$$\frac{dS(t)}{dt} + M(t)S(t) \geq 0. \quad (5)$$

Multiplying Equation (5) by $\exp\left(\int_0^t M(s)ds\right)$, we get

$$\frac{dS(t)}{dt}\exp\left(\int_0^t M(s)ds\right) + M(t)S(t)\exp\left(\int_0^t M(s)ds\right) \geq 0, \quad (6)$$

which implies

$$\frac{d}{dt}\left[S(t)\exp\left(\int_0^t M(s)ds\right)\right] \geq 0. \quad (7)$$

Integrating Equation (7), we have

$$S(t) \geq S(0)\exp\left(-\int_0^t M(s)ds\right). \quad (8)$$

Therefore, the solution $S(t) \geq 0$ for all $t \geq 0$.

Similarly, from the other equations of the system (1a), it is easy to get the following inequalities:

$$L(t) \geq L(0)\exp\left(-\left(\mu + \sum_{i=1}^{n}\gamma_i\right)t\right) \geq 0,$$
$$I_i(t) \geq I_i(0)\exp\left[-(\mu + \delta_i + \alpha_i)t\right] \geq 0, \text{ for } i = 1, 2, \cdots, n \quad (9)$$

$$H(t) \geq H(0)\exp\left[-(\mu + \eta_1 + \rho_1)t\right] \geq 0, \quad (10)$$

$$Q(t) \geq Q(0)\exp\left[-(\mu + \eta_2 + \eta_3 + \rho_2)t\right] \geq 0, \quad (11)$$

and

$$R(t) \geq R(0)\exp\left[-\mu t\right] \geq 0, \quad (12)$$

for all $t \geq 0$. This completes the proof. □

Lemma 2. *For all initial condition (1b), the solution of system (1a) is bounded by the region*

$$\Omega = \left\{(S, L, I_1, I_2, \cdots, I_n, H, Q, R) \in \mathbb{R}_+^{n+5} : S + L + \sum_{i=1}^{n} I_i + H + Q + R \leq \frac{\Lambda}{\mu}\right\}. \quad (13)$$

Proof. From the system (1a), we get

$$\frac{dN(t)}{dt} = \Lambda - \mu N(t) - \sum_{i=1}^{n} I_i\delta_i - \rho_1 H(t) - \rho_2 Q(t). \quad (14)$$

Which implies that

$$\frac{dN(t)}{dt} \leq \Lambda - \mu N(t). \quad (15)$$

Hence,

$$N(t) \leq \frac{\Lambda}{\mu} + N(0)e^{-\mu t}. \quad (16)$$

Thus,

$$\limsup_{t \longrightarrow +\infty} N(t) \leq \frac{\Lambda}{\mu}. \quad (17)$$

□

Lemma 3. *If the initial condition (1b) is satisfied, then the system (1a) admits a unique global solution in $\mathbb{R}_+^{n+5}$.*

Proof. Let us express the model (1a) in the form $Y^{\cdot} = g(Y)$, where

$$cc\,\dot{Y} = \begin{pmatrix} \frac{dS(t)}{dt} \\ \frac{dL(t)}{dt} \\ \frac{dI_i(t)}{dt} \\ \frac{dH(t)}{dt} \\ \frac{dQ(t)}{dt} \\ \frac{dR(t)}{dt} \end{pmatrix}, g(Y) = \begin{pmatrix} \Lambda - \bar{\beta}\frac{S(t)L(t)}{N} - \sum_{i=1}^{n}\frac{\beta_i S(t)I_i(t)}{N} - \mu S(t) \\ \bar{\beta}\frac{S(t)L(t)}{N} + \sum_{i=1}^{n}\frac{\beta_i S(t)I_i(t)}{N} - \left(\mu + \sum_{i=1}^{n}\gamma_i\right)L(t) \\ \gamma_i L(t) - (\mu + \delta_i + \alpha_i)I_i(t) \\ \sum_{i=1}^{n}\sigma\alpha_i I_i(t) - (\mu + \eta_1 + \rho_1)H(t) + \eta_3 Q(t) \\ \sum_{i=1}^{n}(1-\sigma)\alpha_i I_i(t) - (\mu + \eta_2 + \eta_3 + \rho_2)Q(t) \\ \eta_1 H(t) + \eta_2 Q(t) - \mu R(t) \end{pmatrix}. \tag{18}$$

It can be seen easily that the first derivative of g is continuous, then it is locally Lipschitz. According to the fundamental existence and uniqueness theorem [27], Lemma 1 and 2, the system (1a) has a unique positive and bounded solution. □

3. Optimal Control Design

Worldwide, many countries suffer from the pandemic propagation of COVID-19, which result in deaths, infection, and health and economic damage and as consequence, it impacts negatively the individuals and societies. For these reasons, we propose some control strategies which will contribute to reduce the amount of infectious people with strains of COVID-19 $I_i(t)$ for $i \in \{1, 2, \cdots, n\}$, during the time interval $[t_0, t_f]$, and also minimize the cost spent of vaccination and awareness programs.

To achieve these objectives, we provide three control variables. The first control u denotes the effort of the vaccination of susceptible individuals by assuming that all susceptible vaccinated are transferred directly to the removed class. The second control v provides the effort of the awareness programs, security campaigns, and social distancing measures to save the susceptible people (S) from the infection. Hence, the term $(1 - v)$ is introduced to reduce the force of infections. The last control w_i represents the encouraging and diagnosing the infected with i^{th} strain of COVID-19 to join hospitals or quarantined. Then, the system under controls is given by the following system:

$$\begin{cases} \frac{dS(t)}{dt} = \Lambda - \bar{\beta}(1 - v(t))\frac{S(t)L(t)}{N} - \sum_{i=1}^{n}(1 - v(t))\frac{\beta_i S(t)I_i(t)}{N} - \mu S(t) - u(t)S(t), \\ \frac{dL(t)}{dt} = \bar{\beta}(1 - v(t))\frac{S(t)L(t)}{N} + \sum_{i=1}^{n}(1 - v(t))\frac{\beta_i S(t)I_i(t)}{N} - \left(\mu + \sum_{i=1}^{n}\gamma_i\right)L(t), \\ \frac{dI_i(t)}{dt} = \gamma_i L(t) - (\mu + \delta_i + \alpha_i)I_i(t) - w_i(t)I_i(t), \text{ for } i = 1, 2, \cdots, n, \\ \frac{dH(t)}{dt} = \sum_{i=1}^{n}\sigma\alpha_i I_i(t) - (\mu + \eta_1 + \rho_1)H(t) + \eta_3 Q(t) + \chi w_i(t)I_i(t), \\ \frac{dQ(t)}{dt} = \sum_{i=1}^{n}(1-\sigma)\alpha_i I_i(t) - (\mu + \eta_2 + \eta_3 + \rho_2)Q(t) + (1 - \chi)w_i(t)I_i(t), \\ \frac{dR(t)}{dt} = \eta_1 H(t) + \eta_2 Q(t) - \mu R(t) + u(t)S(t), \end{cases} \tag{19}$$

with initial conditions

$$S(0) \geq 0, L(0) \geq 0, I_i(0) \geq 0,$$
$$H(0) \geq 0, Q(0) \geq 0, R(0) \geq 0. \tag{20}$$

Now, we will introduce the optimal control problem, related to the following objective functional:

$$J(u, v, w_i) = \sum_{i=1}^{n} I_i(t_f) + \int_{t_0}^{t_f} \left(\sum_{i=1}^{n} I_i(t) + \frac{A_1}{2} u^2(t) + \frac{A_2}{2} v^2(t) + \sum_{i=1}^{n} \frac{B_i}{2} w_i^2(t) \right) dt, \text{ for } i = 1, 2, \cdots, n \tag{21}$$

where the parameters A_1, A_2, and B_i are strictly positive cost coefficients. They are selected to weigh the relative importance of u, v, and w_i at time t and t_f is the final time.

In other words, we look for optimal controls u, v, and w_i in such a way

$$J(u, v, w_i) = \min_{(u,v,w_i) \in U_{ad}} J(u, v, w_i), \tag{22}$$

for $i = 1, 2, \cdots, n$, with U_{ad} is the set of admissible controls defined by

$$U_{ad} = \left\{ \begin{array}{c} (u(t), v(t), w_i(t)) \colon 0 \leq u(t) \leq 1, 0 \leq v(t) \leq 1, 0 \leq w_i(t) \leq 1, \\ \text{for} i = 1, 2, \cdots, n, \text{and} t \in [t_0, t_f] \end{array} \right\}. \tag{23}$$

3.1. Design of Optimal Controls. In this section, we will use the Pontryagin maximum principle [18, 28] to get the expression of optimal controls and in order to minimize the number of infectious individuals and the cost of control strategies.

Now, Let $\widehat{H}$ be the Hamiltonian defined, in time t, by

$$\widehat{H}(t) = \sum_{i=1}^{n} I_i(t) + \frac{A_1}{2} u^2(t) + \frac{A_2}{2} v^2(t) + \sum_{i=1}^{n} \frac{B_i}{2} w_i^2(t) + \sum_{k=1}^{n+5} \lambda_k f_k, \tag{24}$$

where f_k is the right side of the system (21) of the kth component variable.

Theorem 4. *If the couple $(S^*, L^*, I_1^*, I_2^* \cdots, I_n^*, H^*, Q^*, R^*)$ is the solution of the system (19) related to an optimal control $(u^*, v^*, w_i^*) \in U_{ad}$, then there exist adjoint functions λ_1, λ_2, λ_{i+2}, λ_{n+3}, λ_{n+4}, and λ_{n+5} satisfying the equations:*

$$\begin{cases} \dot{\lambda}_1 = -\dfrac{\partial \widehat{H}}{\partial S} = (\lambda_1 - \lambda_2)\left(\bar{\beta} \dfrac{L(t)}{N} + \displaystyle\sum_{i=1}^{n} \beta_i \dfrac{I_i(t)}{N} \right) + (\lambda_1 - \lambda_{n+5}) u(t) + \mu \lambda_1, \\ \dot{\lambda}_2 = -\dfrac{\partial \widehat{H}}{\partial L} = (\lambda_1 - \lambda_2) \bar{\beta} (1 - v(t)) \dfrac{S(t)}{N} + \lambda_2 \displaystyle\sum_{i=1}^{n} \gamma_i - \gamma_i \lambda_{i+2} + \mu \lambda_2, \\ \dot{\lambda}_{i+2} = -\dfrac{\partial \widehat{H}}{\partial I_i} = -1 + (\lambda_1 - \lambda_2) \displaystyle\sum_{i=1}^{n} \beta_i \dfrac{S(t)}{N} + \gamma_i \lambda_{i+2} - \lambda_{n+3} \displaystyle\sum_{i=1}^{n} \sigma \alpha_i - \lambda_{i+4} \displaystyle\sum_{i=1}^{n} (1 - \sigma) \alpha_i \\ + [\lambda_{i+2} - \chi \lambda_{n+3} - (1 - \chi) \lambda_{n+4}] w_i + (\mu + \delta_i) \lambda_{i+2}, \text{for} i = 1, 2, \cdots, n \\ \dot{\lambda}_{n+3} = -\dfrac{\partial \widehat{H}}{\partial H} = \eta_1 (\lambda_{n+3} - \lambda_{n+5}) + (\mu + \rho_1) \lambda_{n+3}, \\ \dot{\lambda}_{n+4} = -\dfrac{\partial \widehat{H}}{\partial Q} = \eta_3 (\lambda_{n+4} - \lambda_{n+3}) + \eta_2 (\lambda_{n+4} - \lambda_{n+5}) + (\mu + \rho_2) \lambda_{n+4}, \\ \dot{\lambda}_{n+5} = -\dfrac{\partial \widehat{H}}{\partial R} = \mu \lambda_{n+5}, \end{cases} \tag{25}$$

with the transversality conditions at time t_f

$$\lambda_1(t_f) = \lambda_2(t_f) = \lambda_{n+3}(t_f) = \lambda_{n+4}(t_f) = \lambda_{n+5}(t_f) = 0 \text{ and } \lambda_{i+2}(t_f) = 1. \tag{26}$$

Furthermore, for $[t \in t_0; t_f]$, the optimal controls $u^*(t)$, $v^*(t)$, and $w_i^*(t)$ are given by:

$$u^*(t) = \min\left(1, \max\left(0, \frac{(\lambda_1 - \lambda_{n+5}) S(t)}{A_1}\right)\right), \tag{27}$$

$$v^*(t) = \min\left(1, \max\left(0, \cdot \frac{(\lambda_1 - \lambda_2)\left[\bar{\beta}(S(t)E(t)/N) + \sum_{i=1}^{n} \beta_i (S(t) I_i(t)/N)\right]}{A_2}\right)\right), \tag{28}$$

$$w_i^*(t) = \min\left(1, \max\left(0, \frac{[\lambda_{i+2} - \chi\lambda_{i+3} - (1-\chi)\lambda_{i+4}]I_i(t)}{B_i}\right)\right). \tag{29}$$

Proof. The expression of the Hamiltonian $\widehat{H}$ is given as follows

$$\begin{aligned}\widehat{H}(t) = &\sum_{i=1}^{n} I_i(t) + \frac{A_1}{2}u^2(t) + \frac{A_2}{2}v^2(t) + \sum_{i=1}^{n}\frac{B_i}{2}w_i^2(t)\\ &+ \lambda_1\left\{\Lambda - \bar{\beta}(1-v(t))\frac{S(t)L(t)}{N}\right.\\ &\left.- \sum_{i=1}^{n}(1-v(t))\frac{\beta_i S(t)I_i(t)}{N} - \mu S(t) - u(t)S(t)\right\}\\ &+ \lambda_2\left\{\bar{\beta}(1-v(t))\frac{S(t)L(t)}{N} + \sum_{i=1}^{n}(1-v(t))\right.\\ &\left.\cdot\frac{\beta_i S(t)I_i(t)}{N} - \left(\mu + \sum_{i=1}^{n}\gamma_i\right)L(t)\right\}\\ &+ \lambda_{i+2}\{\gamma_i L(t) - (\mu + \delta_i + \alpha_i)I_i(t) - w_i(t)I_i(t)\}\\ &+ \lambda_{n+3}\left\{\sum_{i=1}^{n}\sigma\alpha_i I_i(t) - (\mu + \eta_1 + \rho_1)H(t)\right.\\ &\left.+ \eta_3 Q(t) + \chi w_i(t)I_i(t)\right\} + \lambda_{n+4}\left\{\sum_{i=1}^{n}(1-\sigma)\alpha_i I_i(t)\right.\\ &\left.- (\mu + \eta_2 + \eta_3 + \rho_2)Q(t) + (1-\chi)w_i(t)I_i(t)\right\}\\ &+ \lambda_{n+5}\{\eta_1 H(t) + \eta_2 Q(t) - \mu R(t) + u(t)S(t)\},\end{aligned} \tag{30}$$

for $[t \in t_0; t_f]$. Thanks to Pontryagin's maximum principle, the adjoint equations and transversality conditions can be obtained such that

$$\begin{cases}\dot{\lambda}_1 = -\dfrac{\partial\widehat{H}}{\partial S}, \lambda_1(t_f) = 0,\\ \dot{\lambda}_2 = -\dfrac{\partial\widehat{H}}{\partial E}, \lambda_2(t_f) = 0,\\ \dot{\lambda}_{i+2} = -\dfrac{\partial\widehat{H}}{\partial I_i}, \lambda_{i+2}(t_f) = 1,\\ \dot{\lambda}_{n+3} = -\dfrac{\partial\widehat{H}}{\partial H}, \lambda_{n+3}(t_f) = 0,\\ \dot{\lambda}_{n+4} = -\dfrac{\partial\widehat{H}}{\partial Q}, \lambda_{n+4}(t_f) = 0,\\ \dot{\lambda}_{n+5} = -\dfrac{\partial\widehat{H}}{\partial R}, \lambda_{n+5}(t_f) = 0,\end{cases} \tag{31}$$

for $[t \in t_0; t_f]$. The expression of optimal controls $u^*(t)$, $v^*(t)$, and $w_i^*(t)$ can be given via the optimality condition,

$$\frac{\partial\widehat{H}}{\partial u} = 0, \frac{\partial\widehat{H}}{\partial v} = 0, \text{and} \frac{\partial\widehat{H}}{\partial w_i} = 0. \tag{32}$$

That is

$$\begin{aligned}\frac{\partial\widehat{H}}{\partial u} &= A_1 u(t) + (\lambda_{i+5} - \lambda_1)S(t) = 0,\\ \frac{\partial H}{\partial v} &= A_2 v(t) + (\lambda_2 - \lambda_1)\left[\bar{\beta}\frac{S(t)L(t)}{N} + \sum_{i=1}^{n}\beta_i\frac{S(t)I_i(t)}{N}\right] = 0,\\ \frac{\partial H}{\partial w_i} &= B_i w_i(t) + [-\lambda_{i+2} + \chi\lambda_{i+3} + (1-\chi)\lambda_{i+4}]I_i(t) = 0.\end{aligned} \tag{33}$$

Consequently,

$$\begin{aligned}u^*(t) &= \min\left(1, \max\left(0, \frac{(\lambda_1 - \lambda_{i+5})S(t)}{A_1}\right)\right),\\ v^*(t) &= \min\left(1, \max\left(0, \frac{(\lambda_1 - \lambda_2)\left[\bar{\beta}(S(t)L(t)/N) + \sum_{i=1}^{n}\beta_i(S(t)I_i(t)/N)\right]}{A_2}\right)\right),\\ w_i^*(t) &= \min\left(1, \max\left(0, \frac{[\lambda_{i+2} - \chi\lambda_{i+3} - (1-\chi)\lambda_{i+4}]I_i(t)}{B_i}\right)\right).\end{aligned} \tag{34}$$

By the bounds, in U_{ad}, of the controls, it is easy to obtain $u^*(t)$, $v^*(t)$, and $w_i^*(t)$ in the form of Equations (27), (28), and (29)), respectively. □

4. Numerical Simulation and Discussion

Now, we treat numerically the optimal control problem of the SLI_1I_2HQR model. Here, we obtain the optimality system from the state and adjoint equations. The optimality system is solved by an iterative method. Using an initial guess for the control variables, $u(t)$, $v(t)$, and $w_i(t)$ with (i =1,2), the state variables S, L, I_1, I_2, H, Q, and R are solved forward and the adjoint variables λ_i for $i = 1, 2, 3, 4, 5, 6, 7$ are solved backwards at times step $k = t_0$ and $k = t_f$. If the new values of the state and adjoint variables differ from the previous values, the new values are used to update u_k, v_k, and $w_{i,k}$ (i =1,2) and the process is repeated until the system converges.

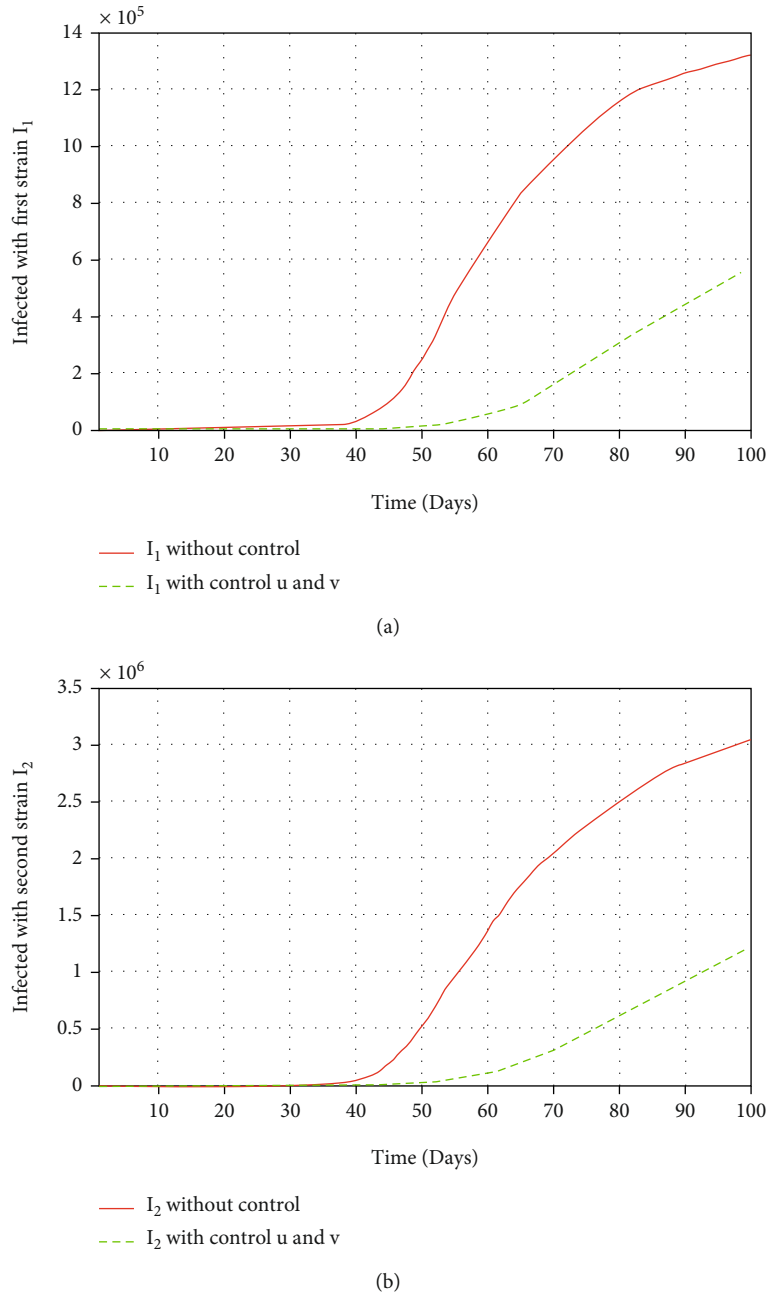

Figure 3: The number of infected individuals with both first (a) and second (b) strain when controls u and v are applied (dashed line), and without controls (solid line).

Based on real data of COVID-19 confirmed cases of the UK, the parameter estimation is made for the first 100 days from 10 Sep 2020 to 10 Jan 2021 (available online at [29]). The total population of the UK is approximately $N = 66.460.344$ and the life expectancy of the UK [30] for the year 2020 is 81. Hence, the natural death rate is calculated to be $\mu = (1/81 * 365)$/per day. Furthermore, at the onset of the pandemic in the UK, only one symptomatic case was confirmed, no individual was confirmed asymptomatic, no hospitalized, and no recovery cases. Consequently, assuming initial number of exposed cases to be 300, the initial number of population is assumed $N(0) = 66.460.344$ where $N(t) = S(t) + L(t) + I_1(t) + I_2(t) + H(t) + Q(t) + R(t)$. The parameter Λ is calculated from the relation $\Lambda = \mu N(t)$ and hence, $\Lambda = 8.175.322$/day, $\sigma = 1/14$/day, $\bar{\beta} = 0.3$,$\beta_1 = 0.4$, $\beta_2 = 0.7$, $\gamma_1 = 0.001$, $\gamma_2 = 0.0019$, $\alpha_1 = 0.04$, $\alpha_2 = 0.03$, $\eta_1 = 0.002$, $\eta_2 = 0.001$, $\eta_3 = 0.002.$, $\delta_1 = 0.0002.$, $\delta_2 = 0.0002.$, $\rho_1 = 0.01.$, $\rho_2 = 0.01$.

Some numerical simulations are presented here in order to illustrate the theoretical results and take into account three control strategies. Then, we consider system (1) with the parameters mentioned above and with initial conditions $S_0 = 66460000$, $L_0 = 300$, $I_{1,0} = 20$, $I_{2,0} = 20$, $H_0 = 3$, $Q_0 = 1$, and $R_0 = 0$.

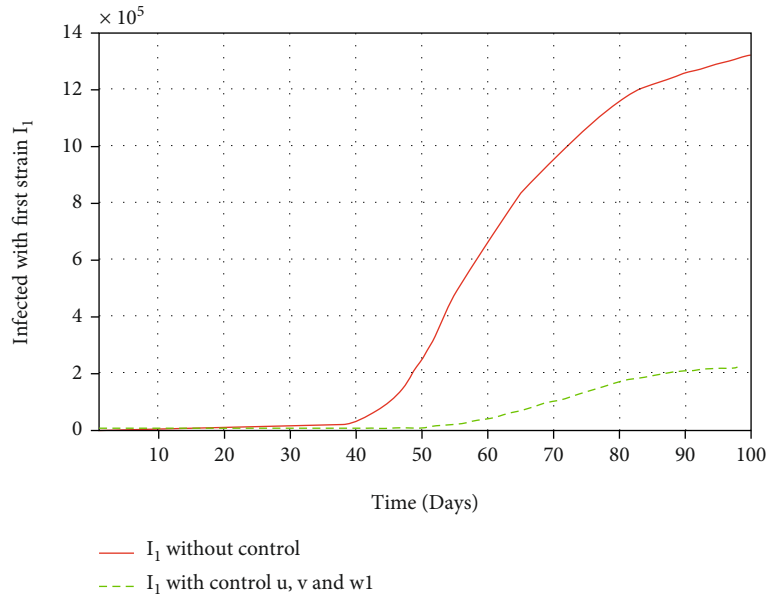

Figure 4: The number of infected individuals with the first strain when controls u, v, and w_1 are applied (dashed line), and without controls (solid line).

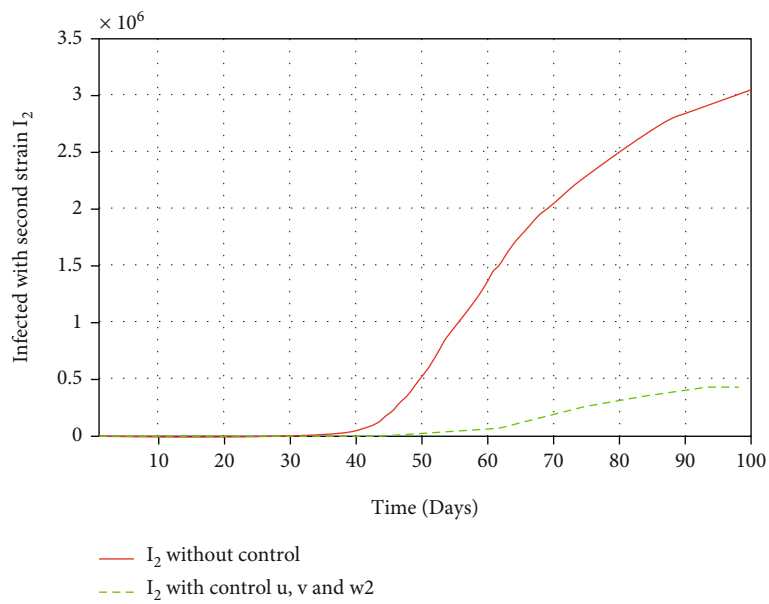

Figure 5: The number of infected individuals with second strain when controls u, v, and w_2 are applied (dashed line) and without control (solid line).

4.1. Strategy 1: Vaccinating Susceptible Individuals and Protecting Them from Contacting Infected Individuals. To realize this objective, we apply only the controls u and v, i.e., vaccinating susceptible individuals having priority who represent individuals with chronic diseases and frontline workers as well as protecting them from contacting infected individuals.

In Figure 3(a), it is observed that there is a significant decrease in the number of infected individuals with the first strain of COVID-19 with control compared to a situation where there is no control which induces a decrease from $1{,}32.10^6$ to $6{,}93.10^5$ at the end of the implementation of the proposed control strategy. Figure 3(b) shows that the number of the infected individuals with second strain of COVID-19 decreased from $3{,}05.10^6$ (without control) to $1{,}54.10^6$ (with control) at the end of the implementation of the proposed control. These changes are important but not sufficient; it is for this reason that we must also add other controls.

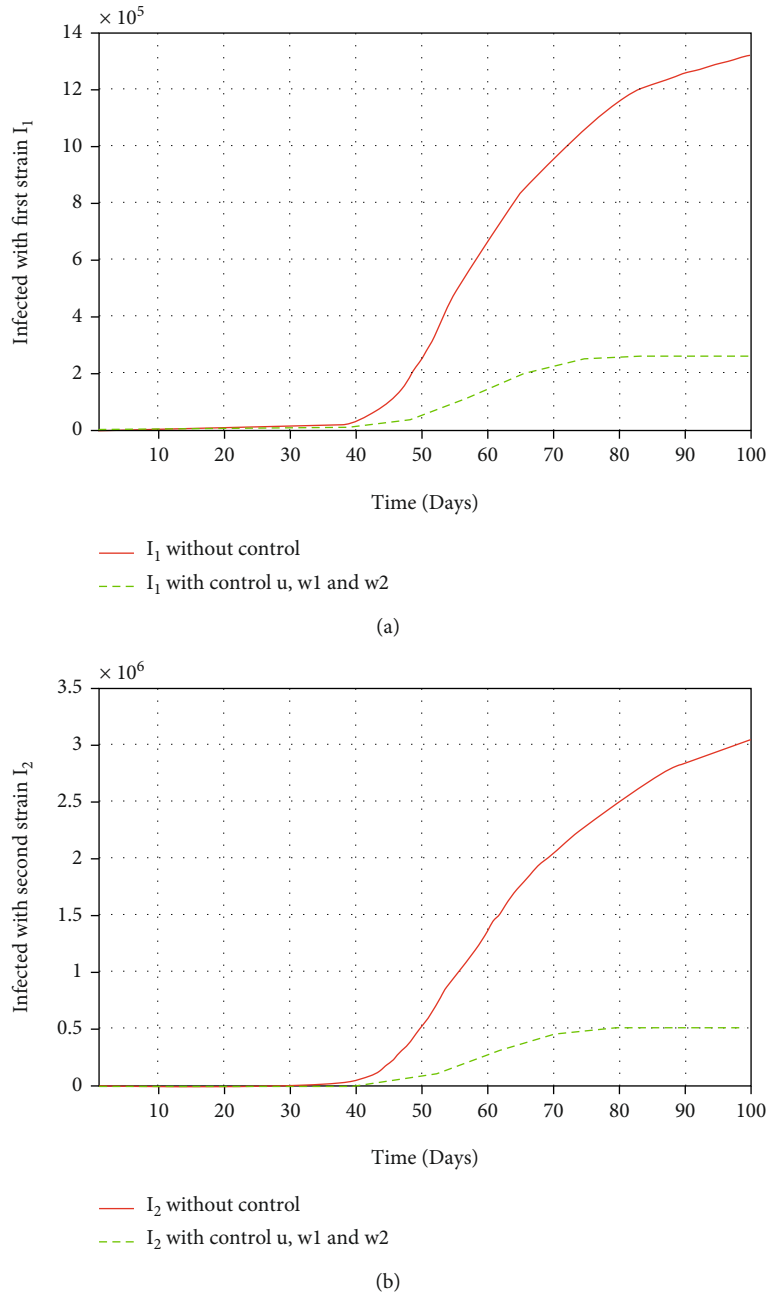

Figure 6: The number of infected individuals with both first (a) and second (b) strain when controls u, w_1, and w_2 are applied (dashed line) and without control (solid line).

4.2. Strategy 2: Vaccinating and Protecting Susceptible Individuals from Contacting Infected Individuals and Encouraging the Symptomatic Infected Individuals with the First Strain of COVID-19 to Go to Hospitals or Do Self-Quarantine. To realize this objective, we apply only the control u, v, and w_1, i.e., vaccinating susceptible individuals having priority who represent individuals with chronic diseases and frontline workers, protecting them from contacting infected individuals, and encouraging the symptomatic infected individuals with the first strain of COVID-19 to go to hospitals or do self-quarantine.

Figure 4 shows that the number of the infected individuals with the first strain of COVID-19 decreases from the value $1{,}32.10^6$ (without controls) to $2{,}206.10^5$ (with controls) at the end of the implementation of the proposed control strategy. As a result, the strategy set before has been achieved.

4.3. Strategy 3: Vaccinating and Protecting Susceptible Individuals from Contacting Infected Individuals and Encouraging the Symptomatic Infected Individuals with the Second Strain of COVID-19 to Go to Hospitals or Do Self-Quarantine. To realize this objective, we apply only the control u, v, and w_2, i.e., vaccinating susceptible individuals having priority who represent individuals with chronic diseases and frontline workers, protecting them from contacting

Table 1: Total costs and total averted infections for strategies 1-4.

Strategy	Total averted infections (TA)	Total cost (TC)
4	$1{,}6829.10^9$	$2{,}9307.10^7$
1	$1{,}9557.10^9$	$3{,}3107.10^8$
2	$2{,}3679.10^9$	$7{,}0051.10^8$
3	$2{,}408.10^9$	$7{,}0632.10^8$

infected individuals, and encouraging the symptomatic infected individuals with the second strain of COVID-19 to go to hospitals or do self-quarantine.

Figure 5 shows that the number of the infected individuals with the second strain of COVID-19 decreases from $3{,}05.10^6$ (without controls) to $4{,}44.10^5$ (with controls) at the end of the implementation of the proposed control strategy. As a result, the strategy set before has been achieved.

4.4. Strategy 4: Vaccinating Susceptible Individuals and Encouraging the Symptomatic Infected Individuals with the First and the Second Strain of COVID-19 to Go to Hospitals or Do Self-Quarantine. To realize this objective, we apply only the control u, w_1, and w_2, i.e., vaccinating susceptible individuals having priority who represent the individuals with chronic diseases and encouraging the symptomatic infected individuals with the first and the second strain of COVID-19 to go to hospitals or do self-quarantine.

Figure 6(a) shows that the number of the infected individuals with first strain of COVID-19 decreases from $1{,}32.10^6$ (without controls) to $2{,}565.10^5$ (with controls) at the end of the implementation of the proposed control strategy. Figure 6(b) shows that the number of the infected individuals with second strain of COVID-19 decreases from $3{,}05.10^6$ (without controls) to $5{,}25.10^5$ (with controls) at the end of the implementation of the proposed control strategy. As a result, the strategy set before has been achieved.

5. Cost-Effectiveness Analysis

In this section, we analyze the cost-effectiveness of the previous four strategies by comparing between them to determine the most cost-effective strategy. Following the method as applied in several studies [31, 32], we evaluate the costs using the incremental cost-effectiveness ratio ($ICER$). This ratio used to compare the differences between the costs and health outcomes of two competing intervention strategies.

The $ICER$ is defined as the quotient of the difference in costs in strategies i and j, by the difference in infected averted in strategies i and $j(i, j \in \{1, 2, 3, 4\})$.

Given two competing strategies E and F, where strategy F has higher effectiveness than strategy $E(TA(F) > TA(E))$, the $ICER$ values are calculated as follows:

$$\begin{aligned} ICER(E) &= \frac{TC(E)}{TA(E)}, \\ ICER(F) &= \frac{TC(F) - TC(E)}{TA(F) - TA(E)}. \end{aligned} \tag{35}$$

The total costs (TC) and the total cases averted (TA) are defined during a given period, for strategy i, with $i = 1, 2, 3, 4$, by:

$$\begin{aligned} TC(i) &= \int_0^{t_f} \big[C_1 u(t)S(t) + C_2 v(t)S(t) \\ &\quad + C_3 w_1(t)I_1(t) + C_4 w_2(t)I_2(t)\big]\,dt, \\ TA(i) &= \int_0^{t_f} \big[(E(t) + I_1(t) + I_2(t)) \\ &\quad - (E^*(t) + I_1^*(t) + I_2^*(t))\big]\,dt, \end{aligned} \tag{36}$$

where C_1, C_2, C_3, and C_4 correspond to the person unit cost of the four possible interventions, while (E^*, I_1^*, I_2^*) is the optimal solution associated to the optimal control (u^*, v^*, w_1^*, w_2^*).

Using the simulation results $(C_1 = C_2 = C_3 = C_4 = 1)$, we ranked in Table 1 our control strategies in order of increased numbers of averted infections.

Strategy 4 is compared with strategy 1 with respect to increased effectiveness and in reference to Table 1. So:

$$\begin{aligned} ICER(4) &= \frac{TC(4)}{TA(4)} = \frac{2{,}9307.10^7}{1{,}6829.10^9} = 0{,}017, \\ ICER(1) &= \frac{TC(1) - TC(4)}{TA(1) - TA(4)} \\ &= \frac{3{,}3107.10^8 - 2{,}9307.10^7}{1{,}9557.10^9 - 1{,}6829.10^9} = 1{,}106. \end{aligned} \tag{37}$$

Strategy 1 is less effective than strategy 4, since $ICER(4) < ICER(1)$. Hence, strategy 1 is eliminated from the set of alternatives.

Next, we compare strategy 4 with strategy 2. The $ICER$ values for strategy 4 and strategy 2 are calculated below:

$$\begin{aligned} ICER(4) &= \frac{TC(4)}{TA(4)} = \frac{2{,}9307.10^7}{1{,}6829.10^9} = 0{,}017, \\ ICER(2) &= \frac{TC(2) - TC(4)}{TA(2) - TA(4)} \\ &= \frac{7{,}0051.10^8 - 2{,}9307.10^7}{2{,}3679.10^9 - 1{,}6829.10^9} = 0{,}979. \end{aligned} \tag{38}$$

Strategy 4 is less effective than strategy 2, since $ICER(2) < ICER(4)$. Consequently, strategy 4 is omitted from the set of alternatives.

Now, we compare strategy 4 with strategy 3. The $ICER$ values for strategy 4 and strategy 3 are calculated below:

$$\begin{aligned} ICER(4) &= \frac{TC(4)}{TA(4)} = \frac{2{,}9307.10^7}{1{,}6829.10^9} = 0{,}017, \\ ICER(3) &= \frac{TC(3) - TC(4)}{TA(3) - TA(4)} \\ &= \frac{7{,}0632.10^8 - 2{,}9307.10^7}{2{,}408.10^9 - 1{,}6829.10^9} = 0{,}933. \end{aligned} \tag{39}$$

Then, strategy 3 is less effective than strategy 4, since $\mathrm{ICER}(4) < \mathrm{ICER}(3)$, Thereafter, strategy 3 is excluded from the set of alternatives.

Hence, we conclude that strategy 4 (vaccinating susceptible people and encouraging the diagnosis of the symptomatic infected individuals with the first and the second strain of COVID-19 to go to hospitals or do self-quarantine) is the most effective strategy.

6. Conclusion

This work proposed a novel deterministic model of COVID-19 taking into consideration multistrain characteristics of the virus and optimal control measures in such a way to minimize the number of infected individuals. Therefore, unlike previous works in the literature, we have taken into account the impact of vaccination, hospitalization, quarantine, and social distancing on multistrains of COVID-19 propagation.

Reducing contact, disinfecting, and imposing quarantine and hospitalization all have substantial influence on the dynamics of COVID-19 propagation and can greatly reduce the spread of multistrain COVID-19. Thus, it is crucial to urge people to take the vaccine and go to hospitals or do self-quarantine. For these reasons, we formulated an optimal control problem based on the proposed model to which we included three control measures: representing vaccination, awareness programs (security campaigns and/or social distancing measures), and diagnosing the infected individuals to join hospital or do self-quarantine. By using the Pontryagin maximum principle, we obtained the expression of the optimal controls which minimize the amount of infectious individuals and the cost of control strategies.

Numerical simulations are carried out in the case of two-strain COVID-19 and with four different control strategies. The optimal strategies including vaccination of susceptible individuals, protection of individuals from being infected with the virus, security campaigns and health measures to prevent the contact of susceptible individuals with infected individuals, and diagnosing the infected with first and second strain i to join hospital or do self-quarantine (strategies 1, 2, 3, and 4) showed significant differences in the number of infections with the first strain and with the second strain, quarantined and hospitalized individuals compared to a situation where no controls are applied. The optimal strategies used have positive effects in decreasing the number of the infected individuals with the first strain and the second strain and also on increasing the number of quarantined individuals. Furthermore, by using the incremental cost-effectiveness ratio method, we show that strategy 4 (vaccinating susceptible individuals and diagnosing the symptomatic infected individuals with the first and the second strain of COVID-19 to go to hospitals or do self-quarantine) is the most effective one.

Data Availability

No data.

Conflicts of Interest

The authors declare that there is no conflict of interest regarding the publication of this paper.

References

[1] I. I. Bogoch, A. Watts, A. Thomas-Bachli, C. Huber, M. U. G. Kraemer, and K. Khan, "Pneumonia of unknown aetiology in Wuhan, China: potential for international spread via commercial air travel," *Journal of Travel Medicine*, vol. 27, no. 2, 2020.

[2] T. M. Chen, J. Rui, Q. P. Wang, Z. Y. Zhao, J. A. Cui, and L. Yin, "A mathematical model for simulating the phase-based transmissibility of a novel coronavirus," *Infectious Diseases of Poverty*, vol. 9, no. 1, pp. 1–8, 2020.

[3] "World Health Organization's 2020 report," http://www.who.int/csr/don/21-december-2020-sars-cov2-variant-united-kingdom/en/.

[4] http://www.statista.comstatistics1101958cumulative-coronavirus-cases-in-the-uk/ (as of Jan 10, 2021).

[5] http://www.statista.comstatistics1101958cumulative-coronavirus-cases-in-the-SouthAfrica (as of January 14, 2021).

[6] B. Khajji, A. Kouidere, M. Elhia, O. Balatif, and M. Rachik, "Fractional optimal control problem for an age-structured model of COVID-19 transmission," *Chaos, Solitons & Fractals*, vol. 143, article 110625, 2021.

[7] B. Khajji, D. Kada, O. Balatif, and M. Rachik, "A multi-region discrete time mathematical modeling of the dynamics of covid-19 virus propagation using optimal control," *Journal of Applied Mathematics & Computing*, vol. 64, no. 1, pp. 255–281, 2020.

[8] A. Kouidere, B. Khajji, A. El Bhih, O. Balatif, and M. Rachik, "A mathematical modeling with optimal control strategy of transmission of covid-19 pandemic virus," *Communications in Mathematical Biology and Neuroscience*, vol. 2020, 2020.

[9] R. Ud Din, A. R. Seadawy, K. Shah, A. Ullah, and D. Baleanu, "Study of global dynamics of COVID-19 via a new mathematical model," *Results in Physics*, vol. 19, article 103468, 2020.

[10] M. Mandal, S. Jana, S. K. Nandi, A. Khatua, S. Adak, and T. Kar, "A model based study on the dynamics of covid-19: prediction and control," *Chaos, Solitons & Fractals*, vol. 136, article 109889, 2020.

[11] M. Z. Ndii, P. Hadisoemarto, D. Agustian, and A. K. Supriatna, "An analysis of Covid-19 transmission in Indonesia and Saudi Arabia," *Communication in Biomathematical Sciences*, vol. 3, no. 1, pp. 19–27, 2020.

[12] D. Kada, A. Kouidere, O. Balatif, M. Rachik, and E. H. Labriji, "Mathematical modeling of the spread of covid-19 among different age groups in morocco: optimal control approach for intervention strategies," *Chaos, Solitons & Fractals*, vol. 141, article 110437, 2020.

[13] A. Kouidere, D. Kada, O. Balatif, M. Rachik, and M. Naim, "Optimal control approach of a mathematical modeling with multiple delays of the negative impact of delays in applying preventive precautions against the spread of the COVID-19 pandemic with a case study of Brazil and cost- effectiveness," *Chaos, Solitons & Fractals*, vol. 142, article 110438, 2021.

[14] M. Elhia, L. Boujallal, M. Alkama, O. Balatif, and M. Rachik, "Set-valued control approach applied to a COVID-19 model with screening and saturated treatment function," *Complexity*, vol. 2020, Article ID 9501028, 15 pages, 2020.

[15] L. Boujallal, M. Elhia, and O. Balatif, "A novel control set-valued approach with application to epidemic models," *Journal of Applied Mathematics and Computing*, vol. 65, no. 1-2, pp. 295–319, 2021.

[16] M. Elhia, O. Balatif, L. Boujallal, and M. Rachik, "Optimal control problem for a tuberculosis model with multiple infectious compartments and time delays," *An International Journal of Optimization and Control: Theories & Applications (IJOCTA)*, vol. 11, no. 1, pp. 75–91, 2021.

[17] T. Y. Miyaoka, S. Lenhart, and J. F. Meyer, "Optimal control of vaccination in a vector-borne reaction–diffusion model applied to Zika virus," *Journal of Mathematical Biology*, vol. 79, no. 3, pp. 1077–1104, 2019.

[18] S. Lenhart and J. T. Workman, *Optimal control applied to biological models*, CRC press, 2007.

[19] E. C. Yuan, D. L. Alderson, S. Stromberg, and J. M. Carlson, "Optimal vaccination in a stochastic epidemic model of two non-interacting populations," *PLoS One*, vol. 10, no. 2, article e0115826, 2015.

[20] T. Britton, E. Pardoux, F. Ball, C. Laredo, D. Sirl, and V. C. Tran, *Stochastic Epidemic Models with Inference*, Springer, Cham, Switzerland, 2019.

[21] O. Khyar and K. Allali, "Global dynamics of a multi-strain SEIR epidemic model with general incidence rates: application to COVID-19 pandemic," *Nonlinear Dynamics*, vol. 102, no. 1, pp. 489–509, 2020.

[22] D. Bentaleb, S. Harroudi, S. Amine, and K. Allal, "Analysis and optimal control of a multistrain SEIR epidemic model with saturated incidence rate and treatment," in *Differential Equations and Dynamical Systems*, pp. 1–17, Springer, 2020.

[23] M. Fudolig and R. Howard, "The local stability of a modified multi-strain SIR model for emerging viral strains," *PLoS One*, vol. 15, no. 12, article e0243408, 2020.

[24] C. P. Bhunu, "Mathematical analysis of a three-strain tuberculosis transmission model," *Applied Mathematical Modelling*, vol. 35, no. 9, pp. 4647–4660, 2011.

[25] C. P. Bhunu, P. Claver, and W. Garira, "A two strain tuberculosis transmission model with therapy and quarantine," *Mathematical Modelling and Analysis*, vol. 14, no. 3, pp. 291–312, 2009.

[26] N. H. Sweilam and S. M. Al-Mekhlafi, "Numerical study for multi-strain tuberculosis (TB) model of variable-order fractional derivatives," *Journal of Advanced Research*, vol. 7, no. 2, pp. 271–283, 2016.

[27] L. Perko, *Differential Equations and Dynamical Systems*, Springer Science & Business Media, 2013.

[28] L. S. Pontryagin, V. Boltyanskii, R. Gamkrelidze, and E. Mishchenko, *The Mathematical Theory of Optimal Processes*, Kn Trirogoff, New York, 1962.

[29] "Wikipedia, the free encyclopedia, COVID-19 pandemic in UK," https://en.wikipedia.org/wiki/COVID-19 pandemic in UK.

[30] UN-world, https://www.macrotrends.net/countries/ranking/population.

[31] F. B. Agusto and I. M. ELmojtaba, "Optimal control and cost-effective analysis of malaria/visceral leishmaniasis co-infection," *PLoS One*, vol. 12, no. 2, article e0171102, 2017.

[32] K. O. Okosun, O. Rachid, and N. Marcus, "Optimal control strategies and cost-effectiveness analysis of a malaria model," *BioSystems*, vol. 111, no. 2, pp. 83–101, 2013.

[33] R. M. Neilan and S. Lenhart, "Optimal vaccine distribution in a spatiotemporal epidemic model with an application to rabies and raccoons," *Journal of Mathematical Analysis and Applications*, vol. 378, no. 2, pp. 603–619, 2011.